JOURNAL OF MATERIALS SCIENCE 26 (1991) 6631–6638

Determination of fibre/matrix interfacial shear strength by an acoustic emission technique

A. N. NETRAVALI, Z.-F. LI, W. SACHSE*
*Departments of Textiles and Apparel, and * Theoretical and Applied Mechanics, Cornell University, Ithaca, NY 14853 USA*

H. F. WU
Alcoa Laboratories, Alcoa Center, PA 15069, USA

The application of acoustic emission (AE) measurements to locate the sources of fracture of a single high-strength fibre embedded in an epoxy matrix which is loaded in tension is described. From the micromechanical model and the fragment length distribution, interfacial shear strength values were calculated. The technique is demonstrated for small-diameter glass and graphite fibres as well as for fibres which exhibit fibrillar fracture, such as Kevlar and PBZT. Good agreement is found between the mean fragment length values obtained by optical and AE measurements for glass and graphite fibres. Values obtained for interfacial shear strength by the AE technique are comparable with those obtained using other techniques.

1. Introduction

Structural composite materials fabricated from epoxy resins and reinforced with high-performance fibres have become increasingly important because of their excellent performance characteristics in terms of their high strength, high modulus and light weight. The properties of such composites, however, depend not only on the strength of the reinforcement or the matrix constituents, but for many of them, also on the characteristics of the fibre–matrix interface.

It is well-known that the fibre–matrix interface plays an important role in achieving superior tensile properties of a composite [1, 2]. The tensile strength of the composite is dependent on the ability of the composite to transfer the tensile load from the broken fibres to the surviving ones through shear in the matrix and the interface. Improvement in the interfacial bond strength may increase a composite's tensile strength, but there may be a decrease in the impact strength and toughness [1, 2]. Alternatively, weak interfacial bonding may encourage energy-absorbing modes of crack propagation and thereby increase fracture toughness of the composite [1].

Among the many possible tests applicable to interfaces, two methods which are most often proposed for measuring the fibre/matrix interfacial shear strength (IFSS) include the fibre pull-out test and the single-fibre composite (SFC) test. The fibre pull-out is popular because of its conceptual simplicity. It is, however, not without difficulty. There are clamping and alignment problems, especially for stiff fibres such as graphite and glass, and there are questions related to the required embedded length of the fibre which makes this test not as straightforward as it first appears [3, 4]. In fact, the meniscus at the point of a fibre's entry into the matrix, makes it sometimes difficult to determine the exact embedded length of the fibre. Nevertheless, the pull-out test has been demonstrated to be an important test procedure for determining fibre/matrix interfacial shear strengths as well as permitting an investigation of fibre/matrix frictional effects [3, 4].

Recently, the microbond test which is a modified version of the pull-out test, has been developed by Miller *et al.* [5]. In this test, a small drop of matrix in the form of a bead is deposited on to the fibre at some point. The fibre with its micro-bead is then mounted in a micro-vice and the fibre is pulled out. Although this test is easy to perform, especially for the purpose of screening materials, there are still several concerns of which a user must be aware. These concerns include the stress concentrations during specimen loading, non-uniform shear stress distribution along the fibre/matrix interface, the geometry of the resin droplet, the position of the droplet in the micro-vice and the effect of strain rate. All of these factors will significantly affect the test results and the scatter in the test data. The details of the theoretical study of the micro-bond method are contained in a recent study by Wu *et al.* [6].

The SFC test is a straightforward experimental procedure for determining the fibre/matrix interfacial shear strengths. The procedure involves fabricating a specimen in which a single fibre is completely embedded along the centreline of a relatively larger dog-bone shaped specimen of matrix material. This single-fibre composite is then strained uniaxially along the fibre axis [8–13]. A requirement of the test is that the strain of matrix fracture is at least three times higher than that of the fibre [9]. When compared to the pull-out

0022–2461/91 $03.00 + .12

test, the fabrication and testing of SFC specimens are relatively straightforward. An additional advantage of the SFC method is that in transparent, photoelastic matrices, the debonding and matrix shear stresses can be observed and analysed with an optical microscope possessing crossed polarizers [12]. As the specimen is loaded, the strain in the specimen increases and the fibre breaks repeatedly, with increasing strain of the specimen, at successive weak points or flaws along its length. Finally, the fibre fragments become so short that the shear transfer along their length can no longer continue to build up the tensile stress to cause additional failures. After this point, no additional breaks occur in the fibre with increased strain and the test is complete [9–11].

Based on a force balance in a micromechanical model for a system of elastic fibre embedded in plastic matrix, sometimes termed a shear lag analysis, Kelly and Tyson [13, 14] argued that the maximum length that a fibre fragment can have, l_c, which is referred to as the critical fragment length, is given by

$$\tau = \frac{d\sigma_f}{2l_c} \tag{1}$$

where τ is the yield shear stress of the interface or the matrix, d is the fibre diameter, and σ_f is the fibre failure stress at the critical length, l_c, which is defined as the maximum fragment length when the fragmentation ceases. The ratio l_c/d is called the critical aspect ratio. A fibre of length greater than l_c could break into two fragments and hence the actual fragment lengths vary between $l_c/2$ and l_c. Some authors have assumed a uniform fragment length distribution with a mean, $\bar{l}$, of 0.75 l_c [15]. This leads to the modified formula

$$\tau = \frac{d\sigma_f}{2\bar{l}}(K) \tag{2}$$

where K is 0.75. Henstenburg and Phoenix [16] recently developed a refined model of the fragmentation process based on a Poisson/Weibull random occurrence of flaws along a fibre and with a linear buildup of the fibre tensile stress away from fibre breaks. They developed a relationship which facilitated the formulation of the model as a Monte Carlo simulation problem in terms of a single factor, the Weibull shape parameter, ρ, for fibre strength. Along with simulating the non-dimensional fibre fragment length distribution, they showed that

$$\tau = \frac{d\sigma_f}{2\bar{l}}\left(\frac{\bar{\Lambda}_\rho}{2}\right)^{(\rho+1)/\rho} \tag{3}$$

where σ_f is the Weibull scale parameter for the fibre strength at a gauge length equal to the mean fragment length, $\bar{l}$. The quantity $\bar{\Lambda}_\rho$ is the non-dimensional mean aspect ratio $(\bar{l}/h)$, where h is a certain characteristic length which is also derived from their model. The analytically inaccessible value of $\bar{\Lambda}_\rho$, can be derived from a Monte-Carlo simulation. The factor $(\bar{\Lambda}_\rho/2)^{(\rho+1)/\rho}$ replaces K in Equation 2. It varies between 0.67 for very large ρ, to 0.97 for $\rho = 3$.

Actual measurements of the fibre fragment lengths are tedious and time consuming. For fibres that exhibit a fibrillar fracture, e.g. polybenzothiozole (PBZT) and aramids such as Kevlar™, fragment length measurements may not be possible. These fibres are known to fracture over a large length, ranging from 20–50 fibre diameters, making it optically difficult to locate the exact fracture point [17, 18]. This can be seen from the photomicrographs of the single Kevlar and PBZT fibres fractured in tension shown in Fig. 1 and the photoelastic stress patterns surrounding the fracture of Kevlar and PBZT fibre fracture (and graphite fibre for comparison) in single-fibre composites shown in Fig. 2a–c, respectively. When opaque matrix materials, such as metals, ceramics, and some polymers are involved, the single fibre breaks are not visible, and so the fragmentation length cannot be determined. An acoustic emission-based measurement provides an alternative.

It has been shown that acoustic emission (AE) signals are generated at every fibre break [19, 20]. These AE signals propagate to the surface of the specimen where they can be detected by one or more sensors. In the case of a single-fibre composite, which can be assumed to be a one-dimensional system and in which the acoustic emission signals are produced only by the fracture of the fibre, it has been possible to locate the position of each break along the length of the fibre by using two sensors along the length of the specimen (and the fibre) and applying a linear source location algorithm to locate the fibre breaks as they occur [20]. Once all the breaks are located, fibre

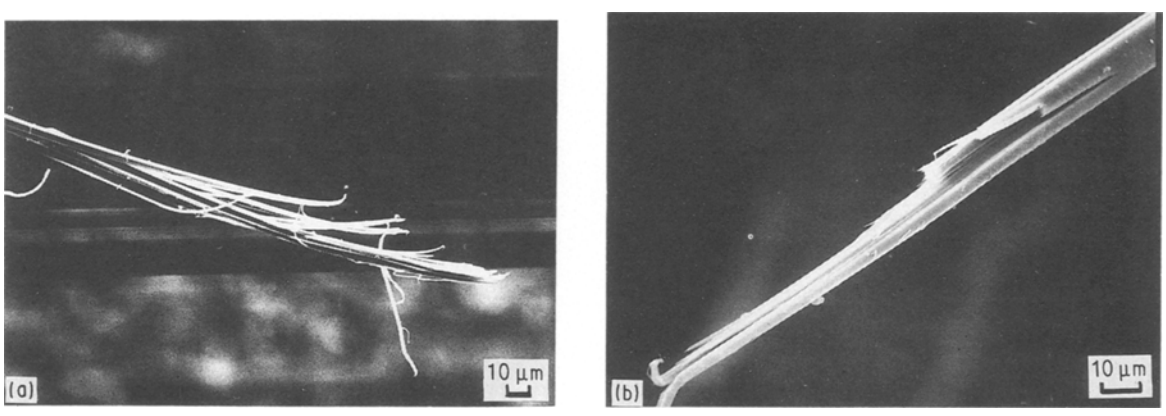

Figure 1 Photomicrographs of (a) Kevlar fibre and (b) PBZT fibre, fractured in simple tension test.

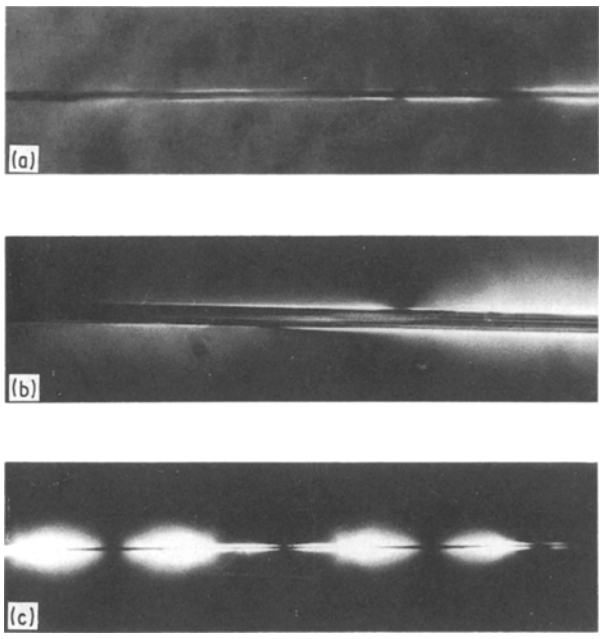

Figure 2 Birefringence patterns at (a) Kevlar fibre break (b) PBZT fibre break and (c) AS-4 graphite fibre break, in SFC specimens.

fragment lengths and thus the aspect ratios can be easily calculated. Petitcorps *et al.* [19] used acoustic emissions to monitor and to count the fibre fractures in SFC specimens of various silicon carbide and boron fibres in a titanium alloy matrix, but they did not use the data to calculate the fragment lengths. Netravali *et al.* [20] used acoustic emissions from fibre breaks to locate the fibre breaks in glass fibre/epoxy SFCs.

In the present paper the work done earlier by Netravali *et al.* [11] on single-fibre composite technique coupled with acoustic emissions from the fibre fracture (SFC/AE) has been extended to measure the fragmentation lengths and thus calculate the interfacial shear stress of small diameter fibres of S-2 glass, AS-4 graphite, and fibres of polybenzothiozole (PBZT) and Kevlar 49 (henceforth called Kevlar) in DGEBA-based epoxy blend. The failure of the latter is characteristically fibrillar in nature. Fragment lengths were also measured optically with a microscope for the specimens containing the S-2 glass and AS-4 graphite fibres. The optical measurements were made to check the accuracy of the acoustic emission technique. The results show good agreement between the mean aspect ratios obtained by AE and optical techniques. The Weibull shape parameter for the AE measurements, however, shows a slightly lower value indicating a higher variation. The interfacial shear strength values for Kevlar fibres are comparable with the values obtained by other workers using other techniques [5, 21].

2. Experimental procedure

2.1. Failure characterization of the fibres

25 single fibres each of S-2 glass, AS-4 graphite, PBZT, and Kevlar were tested in tension in a tensile testing machine using the following procedure. Each fibre, approximately 200 mm long, was divided in half. One section of the fibre was used to determine the linear density using the vibroscope technique according to the procedure defined by ASTM 1577 [12]. Using the measured linear density and knowledge of the volume density of the fibre, the cross-sectional area of the fibre was computed. Published volume densities of 2.49, 1.8, 1.56 and 1.44 g cm^{-3} were used for S-2 glass, AS-4 graphite, PBZT, and Kevlar fibres, respectively. The other half of the fibre was mounted on a paper tab following the modified procedure described in ASTM D3379 [11, 13]. A drop of Permabond 910™ cyanoacrylate cement was used to bond the fibre ends to the tab at a gauge length of 10 mm. All the tests were carried out at 21 °C and 65% r.h. at a strain rate of 0.007 min^{-1}. The failure stress of each fibre was calculated from the cross-sectional area measurement made on that particular fibre's adjacent half.

TABLE I Single-fibre strength parameters

Fibre	Shape parameter	Scale parameter (GPa)
S-2 glass	6.99	4.20
AS-4 graphite	4.91	4.68
PBZT	7.13	3.71
Kevlar	13.98	3.96

The single fibre strength Weibull distribution parameters as determined by the maximum likelihood technique [22] for all four fibres are listed in Table I. The shape parameter governs the variability in strength and the scale parameter is the 62nd percentile of the strength value.

2.2. Single-fibre composite (SFC) specimen preparation

For the fabrication of the SFC specimens, a blend of two epoxies, DER 331, 70% by weight and DER 732, 30% by weight was used. DER 331 is a bisphenol-A based (DGEBA) liquid epoxy with an average epoxy equivalent weight (EEW) of 186. DER 732 is a polyglycol di-epoxide with an average EEW of 320. It was used as a flexibilizer to obtain high fracture strain of the epoxy. The curing agent, DEH 26, was tetraethylenepentamine (TEPA) with an amine hydrogen equivalent weight (AHEW) of 27.1. The epoxies and curing agent were used as -received, without further purification.

To make the blend, epoxy resins, DER 331 and DER 732, were mixed at room temperature and stirred thoroughly to form a homogeneous mixture. The curing agent was then added in stoichiometric proportion. The mixture was stirred again until completely mixed and it was then degassed in a vacuum oven. A silicone rubber mould was used to make the dog-bone shaped SFC specimen, the dimensions of which are shown in Fig. 3. A fibre was held in the central groove of the mould such that the fibre was suspended at half the thickness of the cavity. The epoxy mixture was then slowly poured in, without disturbing the fibre. The mould, with resin and fibre, was then placed in an

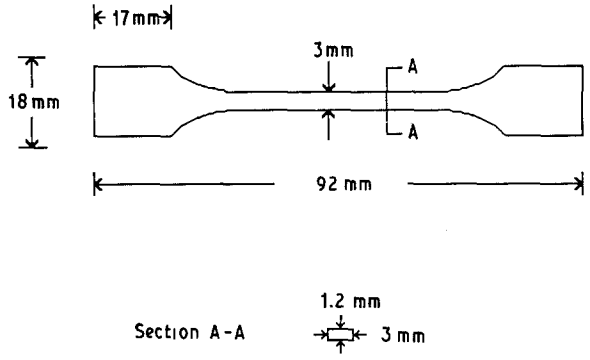

Figure 3 Single-fibre composite (SFC) dog-bone specimen dimensions.

oven for curing. Curing was accomplished at 80 °C for 3 h, after which the oven was turned off and the specimens allowed to cool slowly to room temperature. The cured specimens were then polished to obtain smooth surfaces.

2.3. Single-fibre composite/AE straining apparatus

The dog-bone shaped specimens of the epoxy blends, thus prepared, were strained using a specially constructed AE-instrumented, straining frame. A speed-controlled motor was used to strain the specimens at a constant strain rate of 0.0006 min^{-1}. The elongation of the specimen was monitored by a digital extensiometer interfaced to the data acquisition and processing system. A schematic diagram of the complete setup is shown in Fig. 4.

The acoustic emission signals were detected by miniature piezoelectric transducers whose active area was 1.3 mm^2. The sensors were sensitive to acoustic signals whose frequency ranged from below 10 kHz to above 5 MHz. The output signals from the sensors were amplified by low-noise preamplifiers whose gain was switchable to 40 or 60 dB. In order to be insensitive to the initial portion of the signals having positive or negative slope, the preamplifiers were connected to an amplifying, full-wave rectifier circuit whose gain was an additional 10 dB. The rectified signals were input to a two-channel waveform digitizer and to a high-resolution (20 ps) time-interval counter. The digitizer operated at 10-bit resolution and with a simultaneous digitization rate of 30 MHz. The time interval counter permitted measurement of the time interval between the arrival of the first leading edges of the two signals above a preset threshold level.

2.4. Fibre fragmentation procedure

The SFC specimens containing the fibres were clamped between two grips on the strain frame 60 mm apart and strained until the fibre fragmentation stopped. Two miniature receiver transducers A and B, were held at a fixed distance of 38.1 mm apart for specimens containing S-2 glass, PBZT, and Kevlar fibres and at 25.4 mm apart for specimens containing

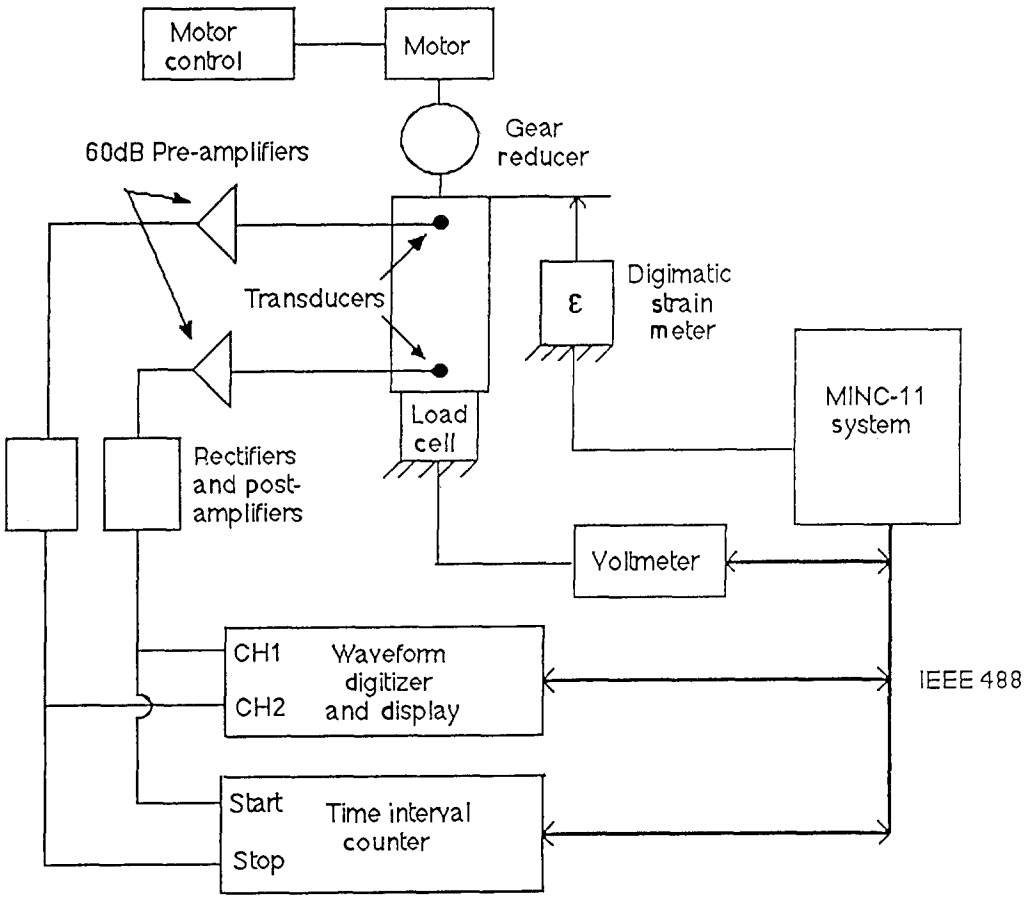

Figure 4 Schematic drawing of the acoustic emission test apparatus for the SFC test.

AS-4 graphite fibres (Fig. 4). The smaller gauge distance for AS-4 fibres was necessary because of the smaller AE signals from these fibres. The running of the test and the data recording proceeded similarly as in our earlier work [20]. Following the test, all the recorded time intervals were processed and evaluated to compute the fragment lengths using the same algorithm developed earlier by Netravali *et al.* [20].

Subsequent to AE tests the specimens containing S-2 glass and AS-4 graphite fibres were observed under an optical microscope equipped with cross-polarizers. Fibre fragment lengths were once again measured with a calibrated eyepiece. The fibre diameter was also measured at four different locations along the length of the fibre. The average diameter was then used to calculate the aspect ratios for the optical as well as the acoustical method. The optical method for fragment length measurement is not usable for the Kevlar or the PBZT fibres because the failure of these fibres extends over a region which is difficult to define from optical measurements. However, the diameters of the fibres were determined using an optical microscope.

3. Results and discussion

Table II is a compilation of the data of fibre diameter, fragment length, aspect ratio, and interfacial shear strength obtained by the optical and AE methods. The fragment length distributions for AS-4 graphite and S-2 glass fibres determined by the AE method were obtained by eliminating a few pairs of fragments that were a combination of a very large and a very small length. This situation arises from the damping of the AE signal observed in the low-modulus epoxy. This makes it sometimes impossible to detect the leading edge of the signal with the time-interval counter thus resulting in an incorrectly determined time interval. This, however, does not affect the mean fragment length values or the mean aspect ratios.

It can be seen from Table II that there is good agreement between the mean values of the aspect ratios obtained by the acoustic and the optical methods for the AS-4 graphite and S-2 glass fibres. Fig. 5a–d shows the Weibull distributions of the aspect ratios for each of the four fibres. The aspect ratios measured by the AE technique in the first 2 mm and the last 2 mm in the gauge length were discarded. This modification is necessary because in the AE testing configuration, the sensors are stationary and as the specimen is strained, it moves under them. As a result, a point on the specimen which is initially outside the gauge length of one sensor, moves insides the gauge length while another point on the specimen which is initially inside the gauge length near the other sensor moves outside the gauge length as the specimen is strained. The result is that not all the fibre breaks occurring approximately within the 2 mm region near the ends of specimen's gauge length are recorded. Hence, the calculated fragment lengths in this region cannot represent the actual fragment lengths. The exclusion of the events at the ends does not lead to a problem, however, since the corresponding fragment lengths are not included because the effective gauge lengths of the specimens were taken as 34.1 mm for S-2 glass, Kevlar and PBZT fibres and 21.4 mm for AS-4 graphite fibres.

For the Kevlar fibres the AE fragment distribution shows that there are a number of fragments which lead to aspect ratios of less than 10. These small fragments referred to as "secondary" fragments corresponded to smaller amplitude AE signals as well. A few secondary fragments were also recorded for PBZT fibres but not as frequently as in the case of Kevlar. The occurrence of these secondary fragments is explained later. For Kevlar fibres three mean values for aspect ratios are shown. The first value, "AE(W)", includes all the detected fragments. In calculating the second value, "AE(A)", secondary fragments were added to the adjacent fragments. The third mean value, "AE(O)", was computed by simply omitting the secondary fragments. The difference between the latter two options is not very significant but when all the fragments are included in the computation, a much smaller mean aspect ratio results, as expected.

A simple model of Kevlar (or PBZT) fibre failure in which the initial fibre break is fibrillar and spread over a large distance is shown in Fig. 6. The fracture crack, which may not be straight, is usually at an angle to the fibre axis. This "primary" break is detected from the

TABLE II Mean aspect ratios, fibre diameters, mean fragment lengths, and interfacial shear strength (IFSS) for different fibres tested

Fibre	Method	Mean aspect ratio	Fibre diameter (μm)	Mean fragment length (mm)	IFSS (MPa)
AS-4 graphite	AE	62.04	7.36	0.46	60.26
	Optical	63.01	7.36	0.46	59.33
S-2 glass	AE	55.62	9.21	0.51	49.26
	Optical	54.31	9.21	0.50	50.59
PBZT	AE	66.27	17.03	1.13	29.31
Kevlar	AE(W)[a]	42.86	11.95	0.51	43.88
	AE(A)[b]	57.61	11.95	0.68	31.98
	AE(O)[c]	52.67	11.95	0.66	35.17

[a] Includes all detected fragments.
[b] Secondary fragments are added to the next fragment.
[c] Secondary fragments are omitted.

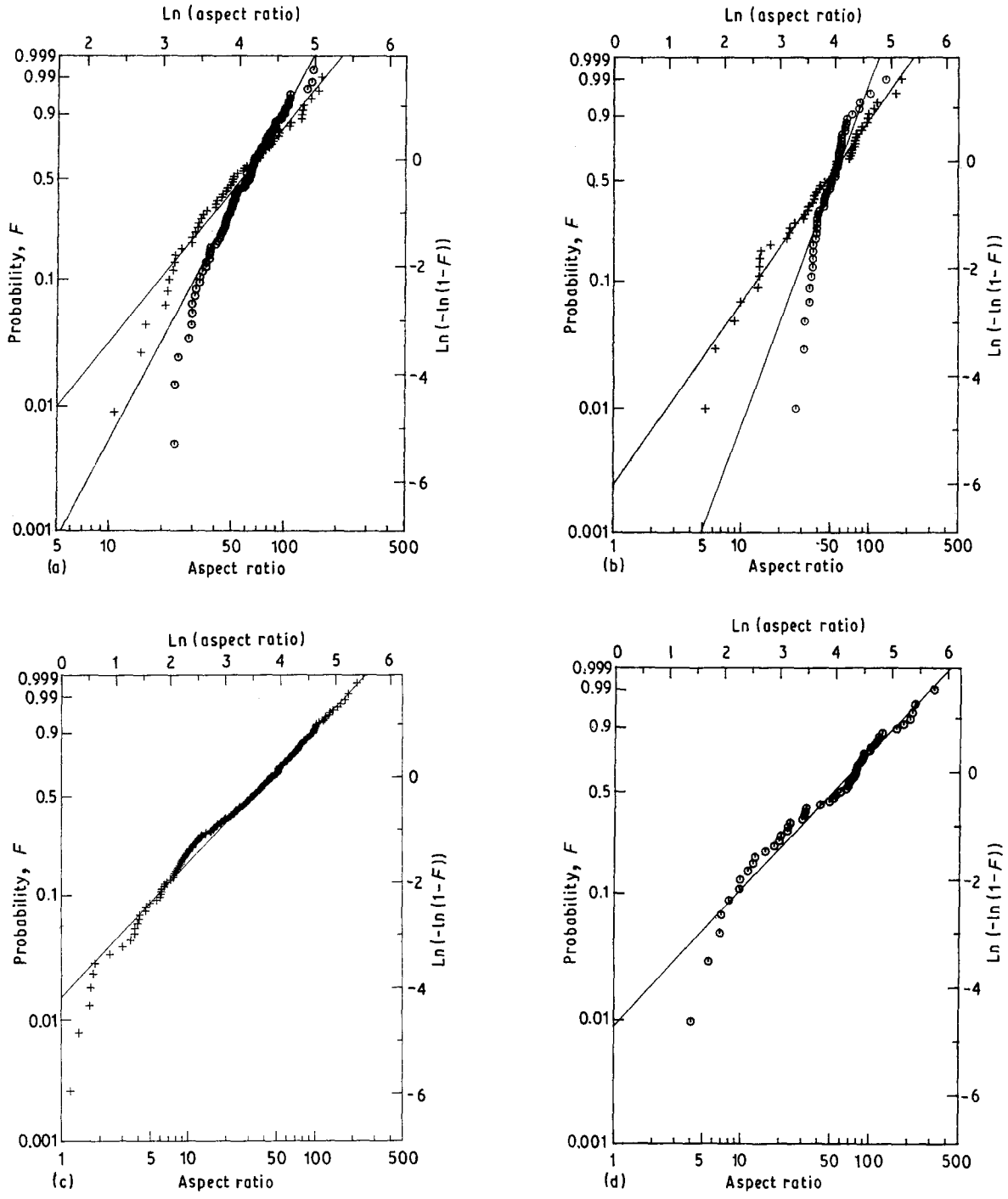

Figure 5 Plots of the aspect ratio distributions of (a) AS-4 graphite fibres and (b) S-2 glass fibres, obtained by (+) the AE method and (○) the optical method on Weibull probability paper. Plots of aspect ratio distributions of (c) Kevlar fibre and (d) PBZT fibre obtained by the AE method.

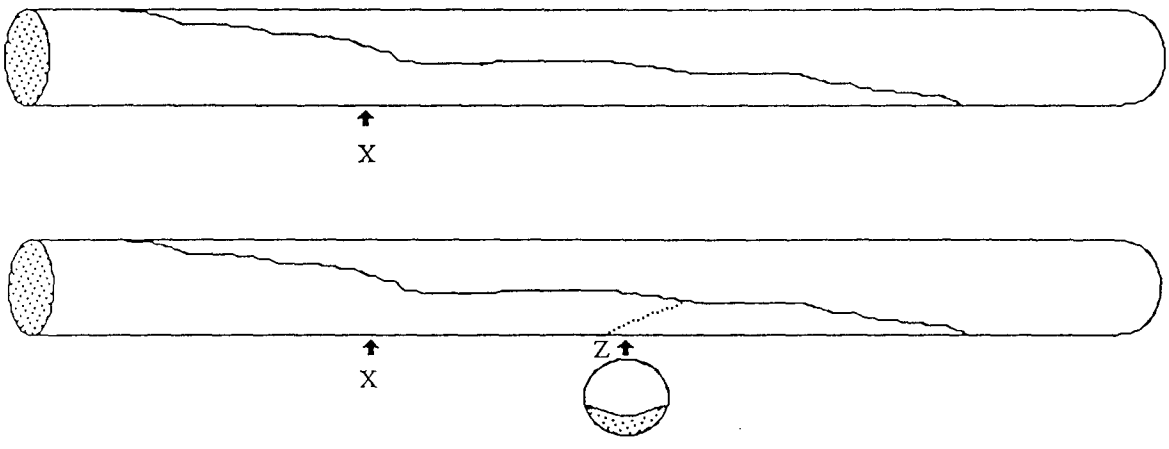

Figure 6 Schematic model of a Kevlar fibre fracture in SFC.

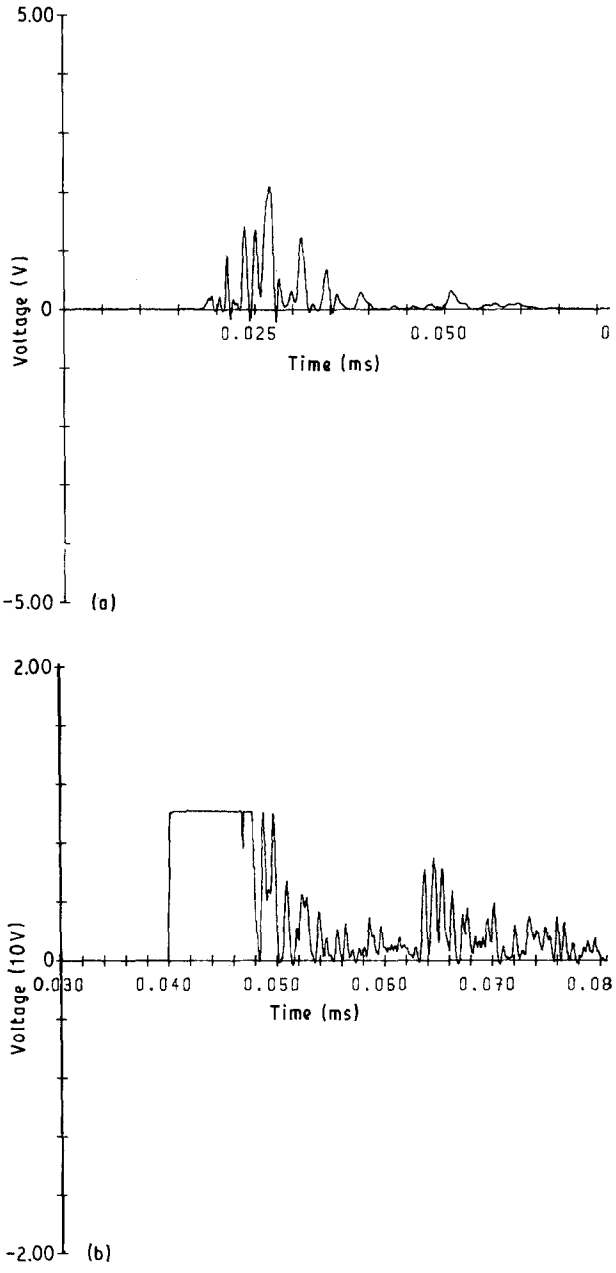

Figure 7 Typical AE signals obtained from Kevlar fibre fracture in SFC. (a) Large amplitude signal. (b) Small amplitude signal.

AE signals at the point marked X where many of the fibrils break. Although the fibre is broken, the interface in the fracture region sometimes appears to fail incompletely. In other words, the fibrils in many cases may still be adhering to the matrix. The occurrence of this depends on several factors, including the type and strength of the bond between the fibre/matrix and the properties of the matrix material. After further straining the SFC specimen, the same fibre (i.e. remaining fibrils still adhering to the matrix) may break at some secondary position, Z, generating additional AE signals and resulting in a secondary fragment of length XZ. Because only a few fibrils break at Z, the emitted AE signal is small. Typical fibre fracture signals at primary and secondary breaks are shown in Fig. 7. The equation for the interfacial shear strength derived by Kelly and Tyson [13] (i.e. Equation 1) or its modified version, Equation 3, can no longer be applied to this situation because only a fraction of the perimeter of the fibre (or the fibrils) is in contact with the matrix and it is impossible to measure the diameter or the cross-sectional area of the broken fibrils. Formation of the secondary fragments in Kevlar or PBZT fibres has, to our knowledge, never been previously reported and was only detected because of the AE technique. For calculating the IFSS it may be appropriate to eliminate these secondary fragments from the fragment length distribution or add to them the neighbouring longer fragments. Indeed, the inclusion of these secondary fragments in the distribution, although done here for comparison, may be incorrect for the reasons stated above. The repeated fracturing of the fibre (or the fibrils) absorbs additional energy and thus adds to the toughness of the composite. Although not done in the present study, it may be possible to estimate, from the amplitude analysis, the fraction of the fibre cross-section involved in the fracture and thus characterize the failure of these fibres.

IFSS values obtained by both the optical and AE methods for S-2 glass and AS-4 graphite and by the AE method for PBZT and Kevlar fibres are also listed in Table II. It is seen that the mean aspect ratios obtained by the two techniques are nearly identical for both AS-4 graphite and S-2 glass fibres which results in nearly identical IFSS values. Thus, the usefulness of AE measurements for small diameter fibres has been demonstrated.

The IFSS value of Kevlar fibres obtained in this study compares well with the IFSS results obtained by other workers of Kevlar fibres in epoxy using other techniques. The IFSS of 32–35 MPa obtained in the present study is comparable to the 33 MPa obtained by Penn *et al.* [21] for this material using the fibre pull-out test and 39 MPa obtained by Miller *et al.* [5] using a microbond technique. The 32–35 MPa, however, is much higher than 17 MPa obtained by Drzal *et al.* [17] using the SFC testing technique but with the fragmentation length determined via optical measurements. In fact, instead of measuring the fragment lengths, Drzal *et al.* [17] measured what they termed the fracture "regions". These fracture regions, apparently, do not exactly correspond to the fragment lengths and hence give a low value of IFSS. The IFSS value of 29.3 MPa obtained in the present study for PBZT in epoxy is also much higher than 10.3 MPa obtained by Drzal [18] for a similar material.

4. Conclusions

Successful measurement of fragment lengths using acoustic emissions from individual fibre breaks to locate the sources of fracture in a single-fibre composite has been shown possible for small-diameter fibres such as AS-4 graphite (7.4 μm, nominal diameter) and S-2 glass fibres (9.2 μm, nominal diameter). The technique also has been successful for Kevlar and PBZT fibres which break in fibrillar manner and are thus normally impossible to measure by conventional optical methods. For S-2 glass and AS-4 graphite fibres the results obtained by optical and AE methods are in close agreement with each other. For the epoxy

blend used, there is a significant amount of damping of the AE signals before they reach the AE sensors. This damping sometimes makes it difficult to detect the leading edge of the AE signal which can result in a significant error in the determination of the individual fragment lengths, though the mean fragment length is not affected. The Kevlar/epoxy interfacial shear strength values obtained by the SFC/AE method are in good agreement with the values obtained by other workers using other techniques. The SFC/AE method can also characterize the "secondary" fragments which are created during the fibrillar fracture of Kevlar and PBZT fibres. The method, as it currently stands, is automated, requires minimal supervision to carry out and is suitable for applications in an industrial environment.

Acknowledgement

This work was supported, in part, by a grant from the ALCOA and the ALCOA Foundation. Support was also derived from the Office of Naval Research (Solid Mechanics Program) under Contract N00014-85-K-0595. The use of the facilities of the Materials Science Center, Cornell University, which is funded by the National Science Foundation is also acknowledged. Special thanks are due to Dr T. E. Helminiac, Wright Patterson Air Force Base, for providing us PBZT fibres to test.

References

1. C. C. CHAMIS, in "Interfaces in Polymer Matrix Composites", edited by E. P. Pluddemann (Academic Press, New York, 1974) pp. 31–77.
2. M. R. PIGGOTT, in "Progress in Science and Engineering of Composites", Proceedings of the 4th International Conference on Composite Materials (1982) p. 193.
3. P. S. CHUA and M. R. PIGGOTT, *Compos. Sci. Tech.* **22** (1985) 33.
4. *Idem., ibid.* **22** (1985) 185.
5. B. MILLER, P. MURI and L. REBENFELD, *ibid.* **28** (1987) 17.
6. H. F. WU, C. M. CLAYPOOL and R. L. ROLF, unpublished data.
7. L. T. DRZAL, M. J. RICH and P. F. LLOYD, *J. Adhes.* **16** (1982) 1.
8. L. T. DRZAL, M. J. RICH, M. F. KOENIG and P. F. LLOYD, *ibid.* **16** (1983) 133.
9. S. H. OWN, R. V. SUBRAMANIAN and S. C. SAUNDERS, *J. Mater. Sci.* **21** (1986) 3912.
10. W. D. BASCOM and R. M. JENSEN, *J. Adhes.* **19** (1986) 219.
11. A. N. NETRAVALI, R. B. HENSTENBURG, S. L. PHOENIX and P. SCHWARTZ, *Polym. Compos.* **10** (1989) 226.
12. A. N. NETRAVALI, S. L. PHOENIX and P. SCHWARTZ, *Polym. Compos.* **10** (1989) 385.
13. A. KELLY and W. R. TYSON, *J. Mech. Phys. Solids* **13** (1965) 329.
14. A. KELLY, *Proc. R. Soc. Lond.* **A319** (1970) 19.
15. A. S. WIMOLKIATISAK and J. P. BELL, *Poly. Compos.* **10** (1989) 162.
16. R. B. HENSTENBURG and S. L. PHOENIX, *Poly. Compos.*, **10** (1989) 385.
17. L. T. DRZAL, in "15th National SAMPLE Technical Conference" (1983) p. 190.
18. *Idem.*, "The Interfacial and Compressive Properties of Polybenzothiozole Fibers", Report AFWAL-TR-86-4003, June 1986.
19. Y. L. PETITCORPS, R. PAILER and R. NASLAIN, *Compos. Sci. Tech.* **35** (1989) 207.
20. A. N. NETRAVALI, L. T. TOPOLESKI, W. H. SACHSE and S. L. PHOENIX, *ibid.* **35** (1989) 13.
21. L. PENN, F. BYSTRY, W. KARP, and S. LEE, in "Molecular Characterization of Composite Interfaces", edited by H. Ishida and G. Kumar (Plenum Press, New York, 1984).
22. A. C. COHEN, *Technometrics* **7** (1965) 597.

Received 30 January
and accepted 19 November 1990